Incorporation of the Tight Binding Hamiltonian into Quantum Liouville-type Equations

Alan Abdi, Mathias Pech and Dirk Schulz
TU Dortmund University, Chair for High Frequency Techniques, Germany
Contact: *alan.abdi@tu-dortmund.de*

Motivation

Quantum Liouville Type Equation:
- ✓ Time-resolved capabilities
- ✓ Inclusion of Scattering

Tight Binding Model:
- ✓ Multiband models
- ✓ FinFETs, RITD, Graphene, …
- ✓ Energy Dispersion

Inclusion of Tight Binding Model into QLTE

Concept

$$i\hbar\frac{\partial\rho}{\partial t} = [H, \rho].$$

Density matrix

$$\boxed{\rho = |\Psi(n)\rangle\langle\Psi(m)| = \sum_n c_n|\phi_n\rangle \sum_m c_m^\dagger\langle\phi_m|\,.}$$

TB-Hamiltonian

$$\boxed{H = \sum_n \epsilon_n|\phi_n\rangle\langle\phi_n| + \sum_{\langle n,m\rangle} \gamma_{nm}|\phi_n\rangle\langle\phi_m|}$$

ϕ :=orbital functions

Concept

Idea: Multiplication with $\langle\phi_l|$ from the l.h.s. and with $\phi_k\rangle$ from the r.h.s.

$$\sum_{n,m}\langle\phi_l|\phi_n\rangle\langle\phi_m|\phi_k\rangle i\hbar\frac{\partial}{\partial t}c_n c_m^\dagger = \langle\phi_l|\sum_{n,m}c_n H|\phi_n\rangle\, c_m^\dagger\langle\phi_m|\phi_k\rangle - \sum_{n,m}c_n\langle\phi_l|\phi_n\rangle\langle\phi_m H\, c_m^\dagger|\phi_k\rangle$$

Exploiting the orthogonalities:

$$\langle n|H|m\rangle = \begin{cases}\epsilon_s, & n=m\\ \gamma, & n=m\pm 1\\ 0, & \text{otherwise}\end{cases}$$

$$\Rightarrow\quad i\hbar\frac{\partial}{\partial t}C_{lk} = \sum_n d_{nm}C_{lk} - \sum_m d_{nm}C_{lk} + (V_n - V_m)C_{lk}$$

Center mass transformation

Center mass transformation onto χ and ξ-coordinates

$$\mathbf{C}_{\chi,\xi} = \mathbf{D_f} \cdot \mathbf{C}_{\chi^{\mathrm{mid}},\xi^{mid}} - \mathbf{V_f} \cdot \mathbf{C}_{\chi,\xi}$$

Coupled grids

$$\mathbf{C}_{\chi^{mid},\xi^{mid}} = \mathbf{D_g} \cdot \mathbf{C}_{\chi,\xi} - \mathbf{V_g} \cdot \mathbf{C}_{\chi^{\mathrm{mid}},\xi^{\mathrm{mid}}}$$

Taylor expansion of $C_{\chi^{mid},\xi^{mid}}$, around χ, ξ $\xrightarrow{\Delta\chi,\Delta\xi \to 0}$ Wigner Equation

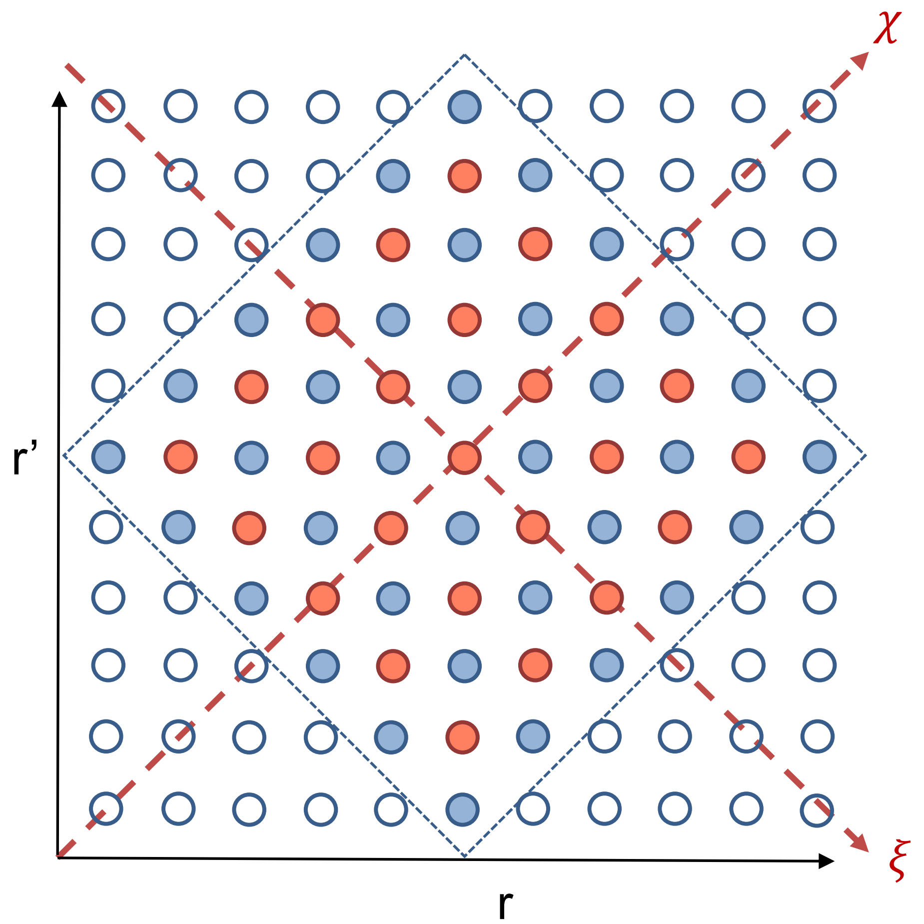

Fig. 1: Elements of the Density Matrix after the center mass Transformation.

Plane wave expansion

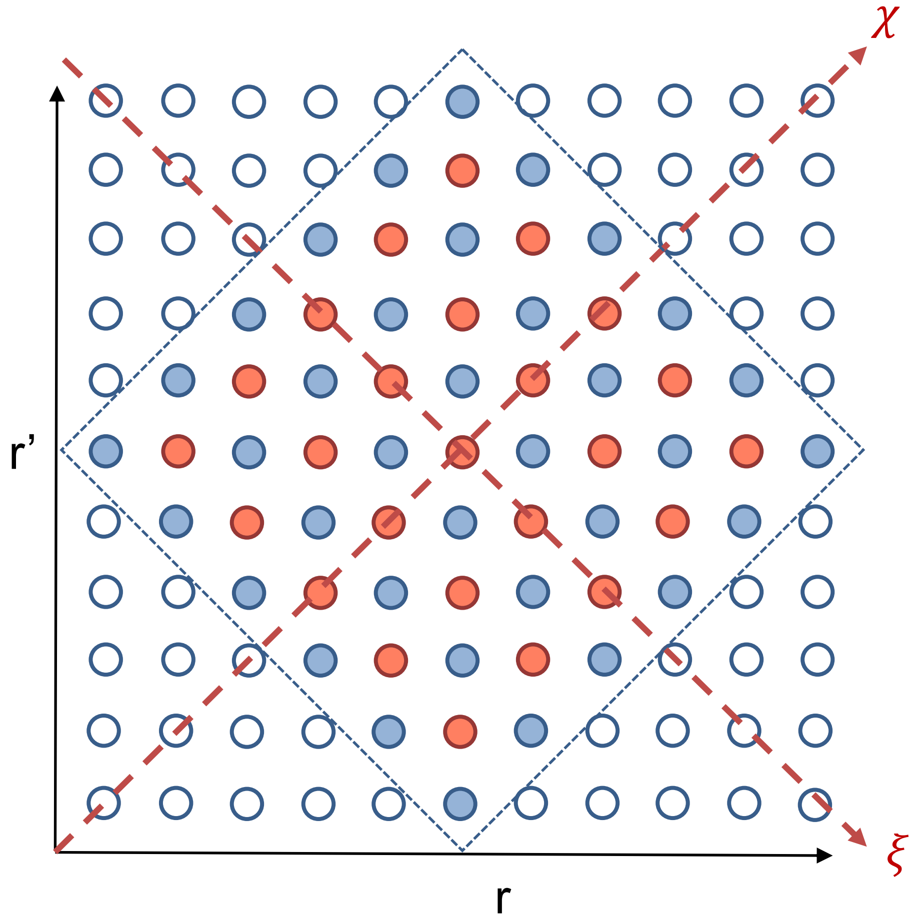

Fig. 1: Elements of the Density Matrix after the center mass Transformation.

Plane wave expansion in ξ-direction (basis $\boldsymbol{\Phi_F}$ and $\boldsymbol{\Phi_G}$)

$$i\hbar\frac{\partial}{\partial t}f_{\chi,k}=(\boldsymbol{\Phi}_G^{\dagger}\boldsymbol{D}_f\boldsymbol{\Phi}_F)g_{\chi,k}-(\boldsymbol{\Phi}_F^{\dagger}\boldsymbol{V}_F\boldsymbol{\Phi}_F)f_{\chi,k}$$

$$i\hbar\frac{\partial}{\partial t}g_{\chi,k}=(\boldsymbol{\Phi}_F^{\dagger}\boldsymbol{D}_g\boldsymbol{\Phi}_G)f_{\chi,k}-(\boldsymbol{\Phi}_G^{\dagger}\boldsymbol{V}_G\boldsymbol{\Phi}_G)g_{\chi,k}$$

Discussion I: Verification (RTD)

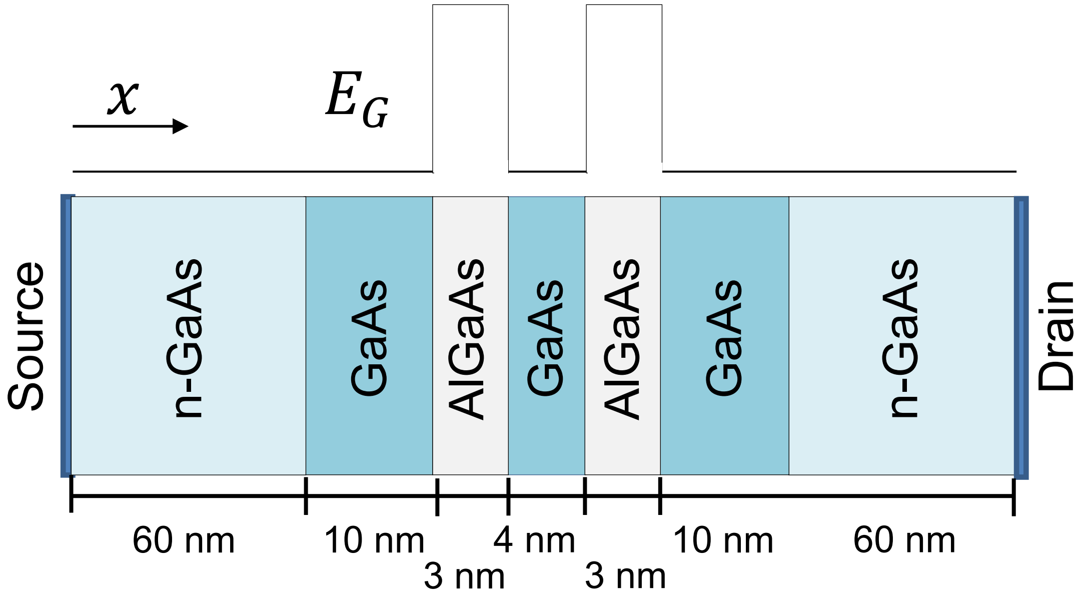

Fig. 2: Schematic of the RTD device assuming homogenous effective mass and 1-dimensional transport.

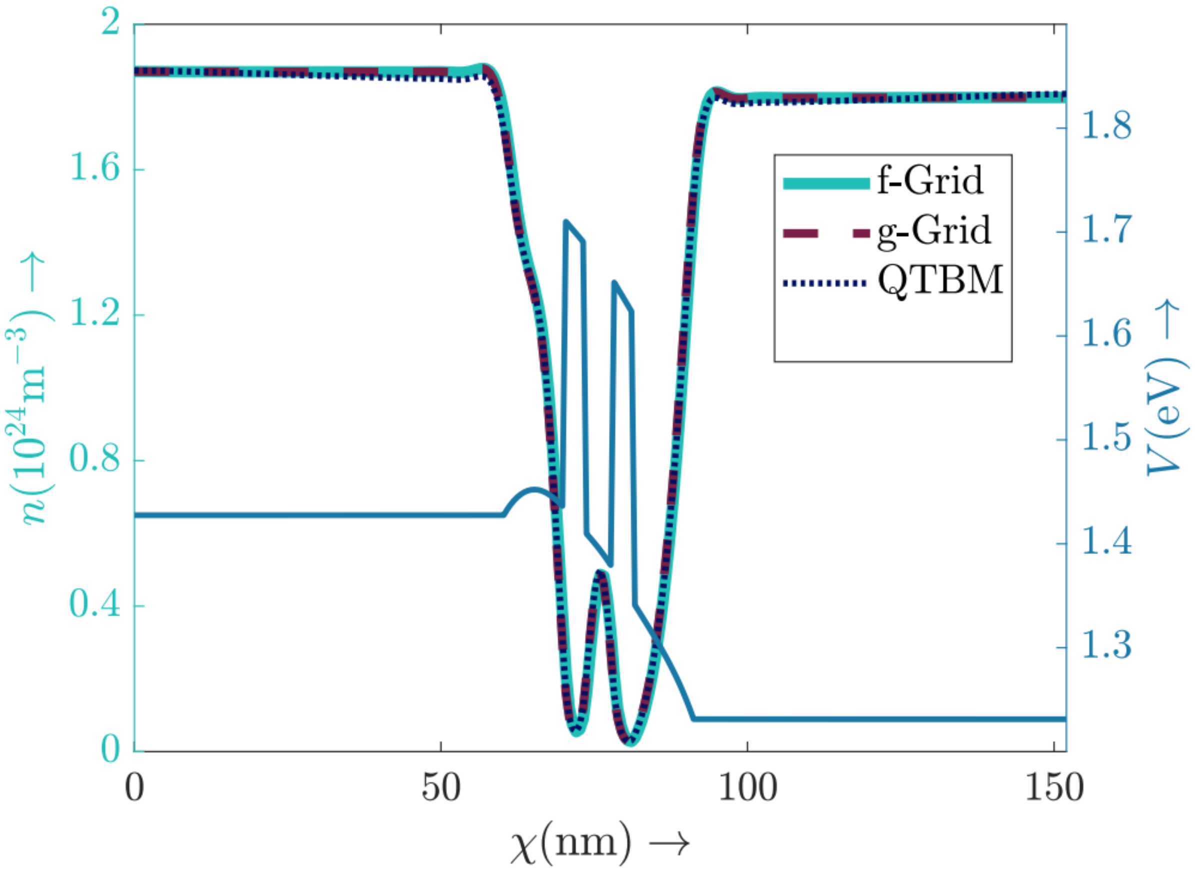

Fig. 3: The self-consistent potential and charge carrier densities for a RTD when a drain voltage of 0.2 V is applied.

Excellent agreement with QTBM
(Quantum Transmitting Boundary Method)

Discussion II: Comparison (QTBM)

- ✓ Good convergence throughout NDR region
- ✗ Complex absorbing potential (CAP) critical

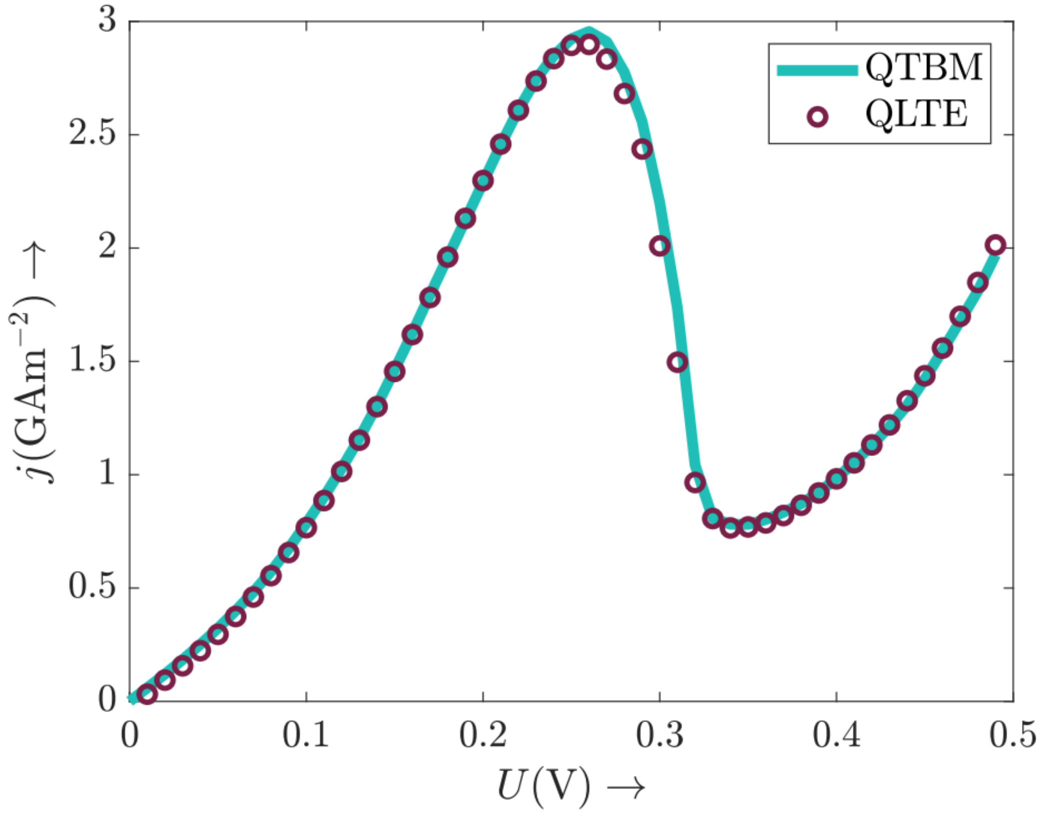

Fig. 4: The mean drain-end current density of grids f and g converges towards the contacts.

Discussion III: Comparison (conventional Wigner)

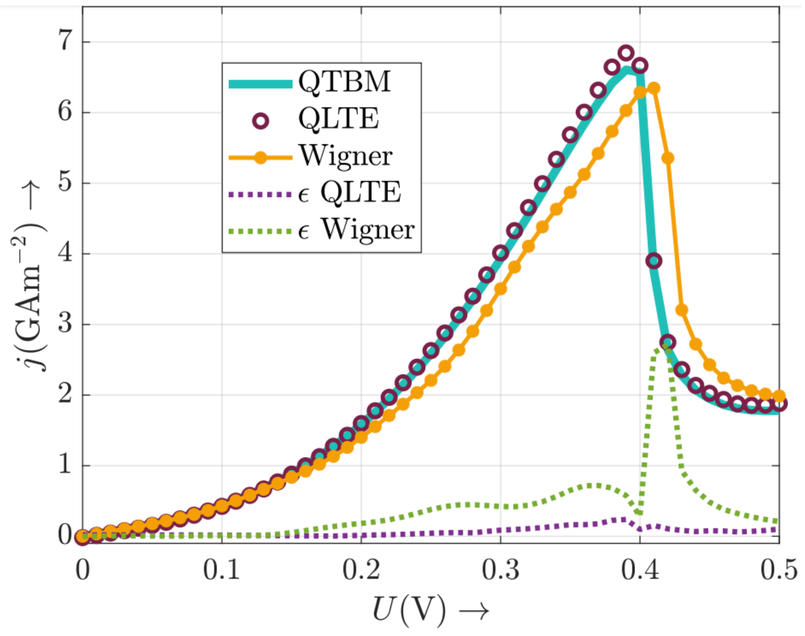

(a) short device (110nm)

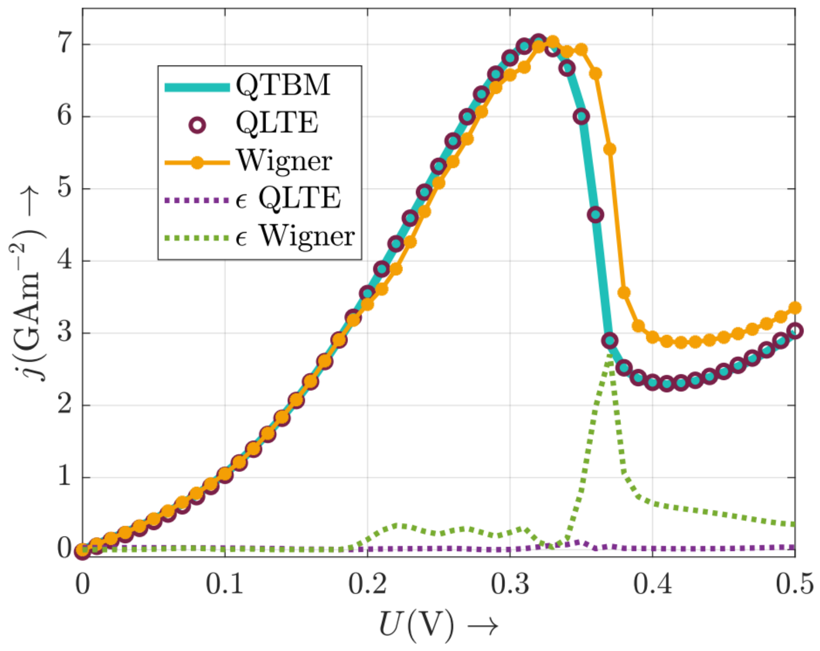

(b) long device (150nm)

Fig. 5: Steady state I-V curves are shown applying the QTBM, the conventional WTE and the proposed approach (QLTE). The current density is shown dependent on the applied voltage U and for two differently dimensioned test devices (shortened contacts).

Discussion IV: Complex Absorbing Potential

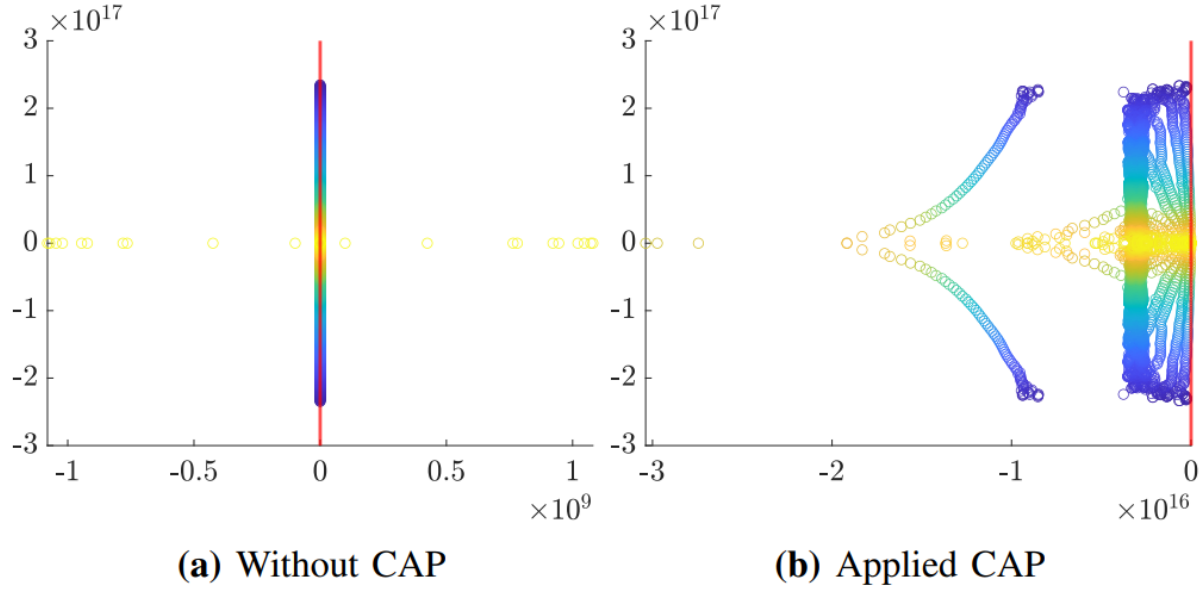

Fig. 6: Eigenvalues of the system matrix on the complex plane.

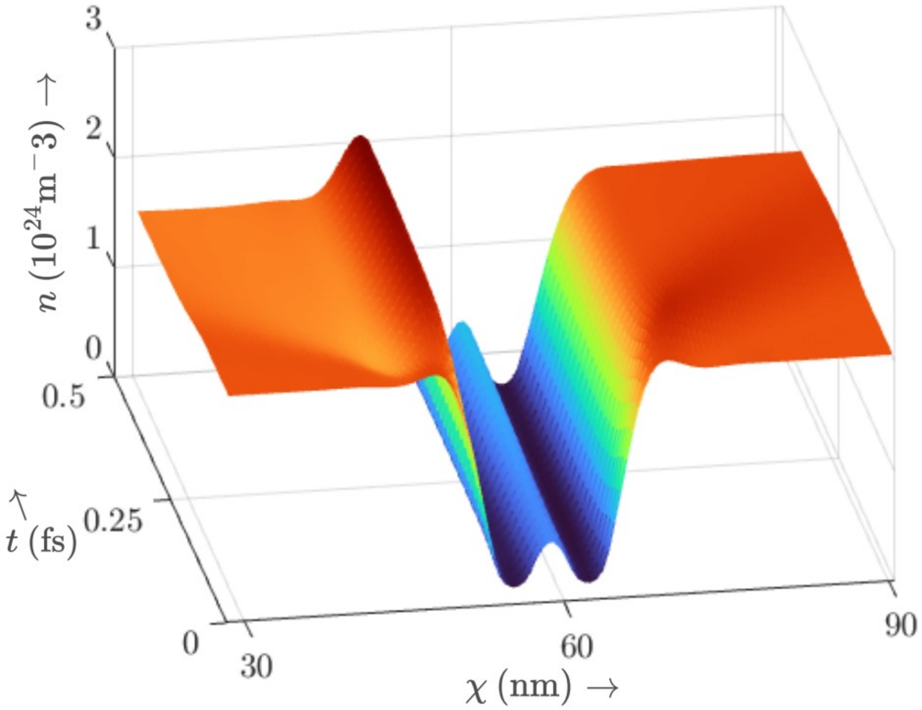

Fig. 7: Spatially time dependent carrier density n_f.

The CAP shifts the eigenvalues to the left half plane

Discussion V: Energy Dispersion

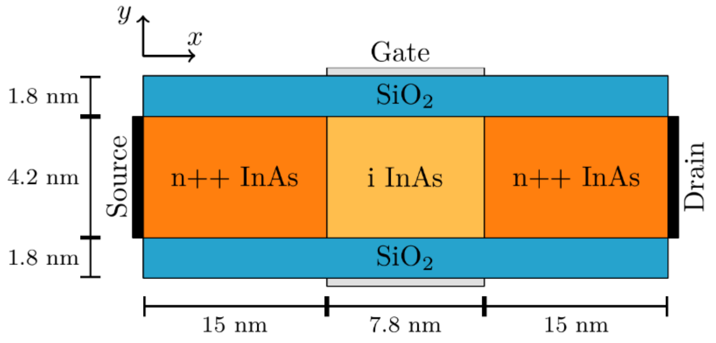

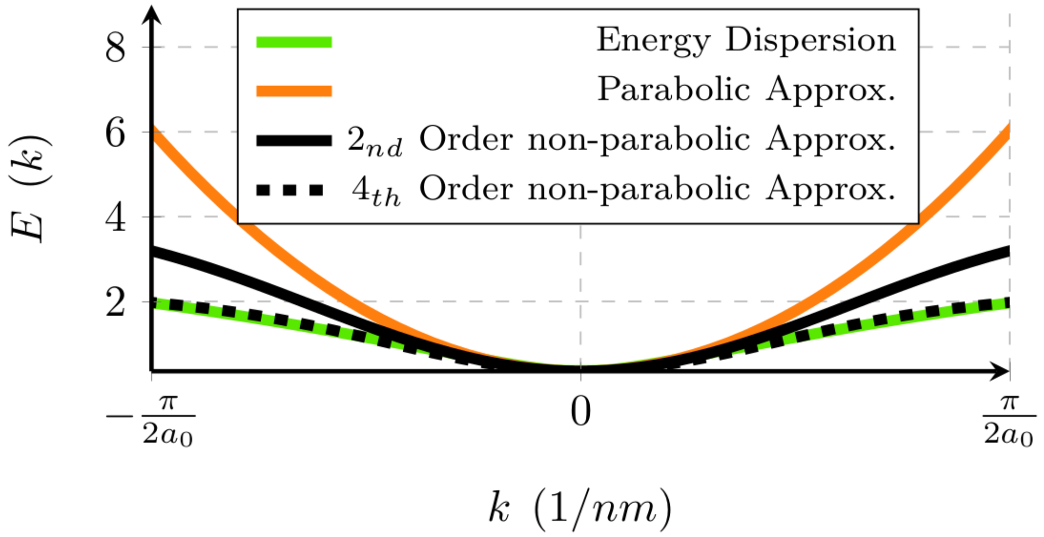

Fig. 8: Bulk energy dispersion in the Γ valley for InAs with parabolic, second order and fourth order approximations.

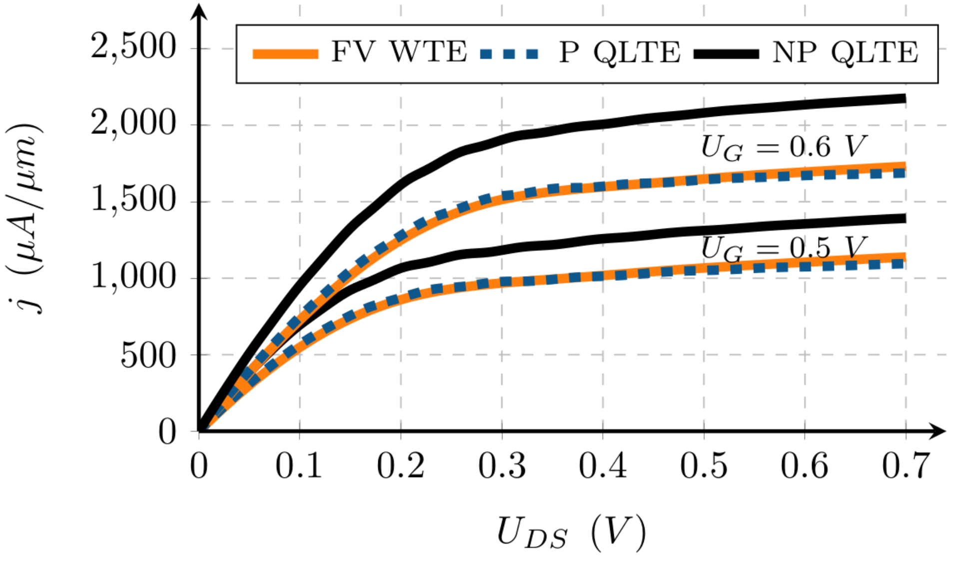

Fig. 9: Drain end current densities for finite volume Wigner, parabolic QLTE and second order non-parabolic QLTE.

Summary

The presented approach is …

- ✓ … a two staggered grid formalism based on WTEs
- ✓ … independent of any discretization patterns (FD, FV,…)
- ✓ … in good accordance with reference solutions
- ✓ … predestined for extension to more complex problems

- ✗ … in need for improved boundary conditions!

www.tu-dortmund.de

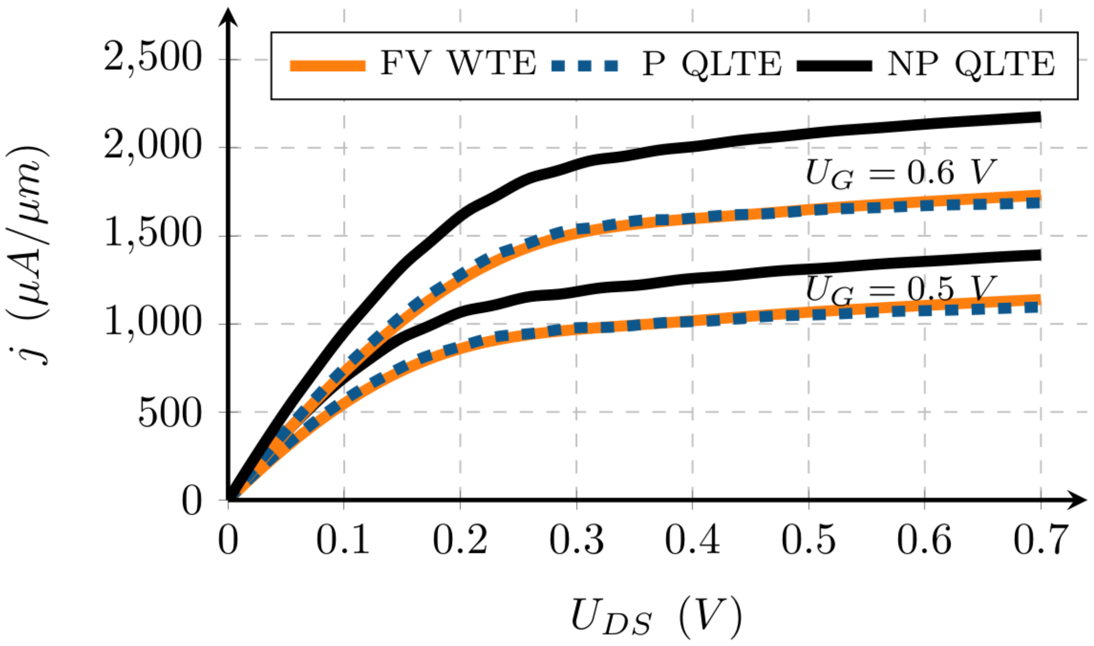

Fig. 10: Drain end current densities for finite volume Wigner, parabolic QLTE and second order non-parabolic QLTE.

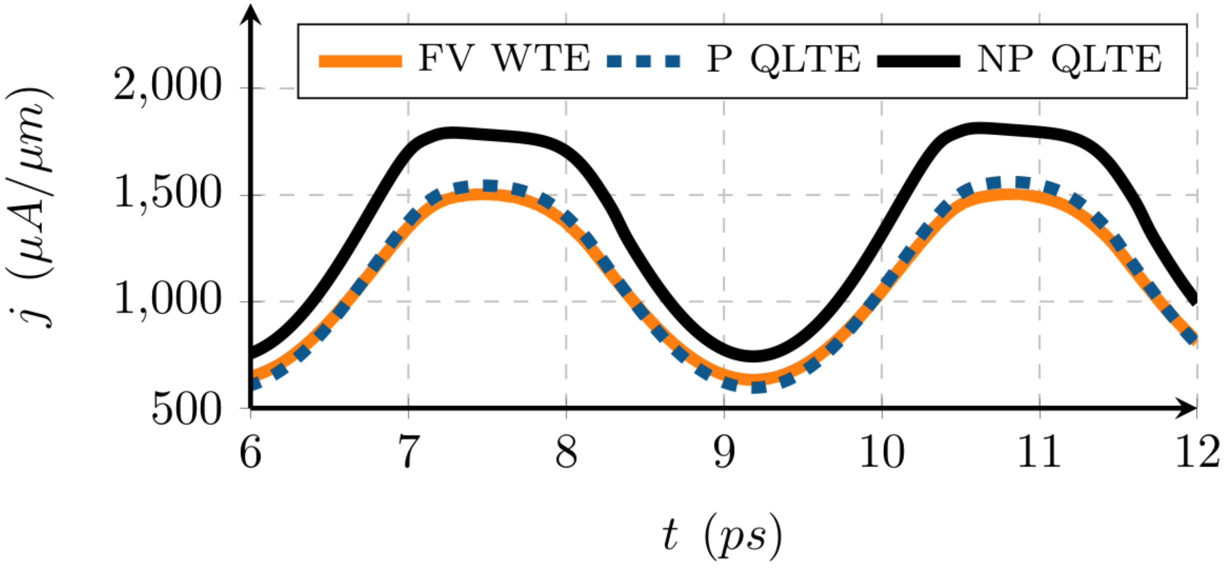

Fig. 11: Time resolved drain-end current densities for the same cases when a harmonic gate voltage at 300 GHz is applied.

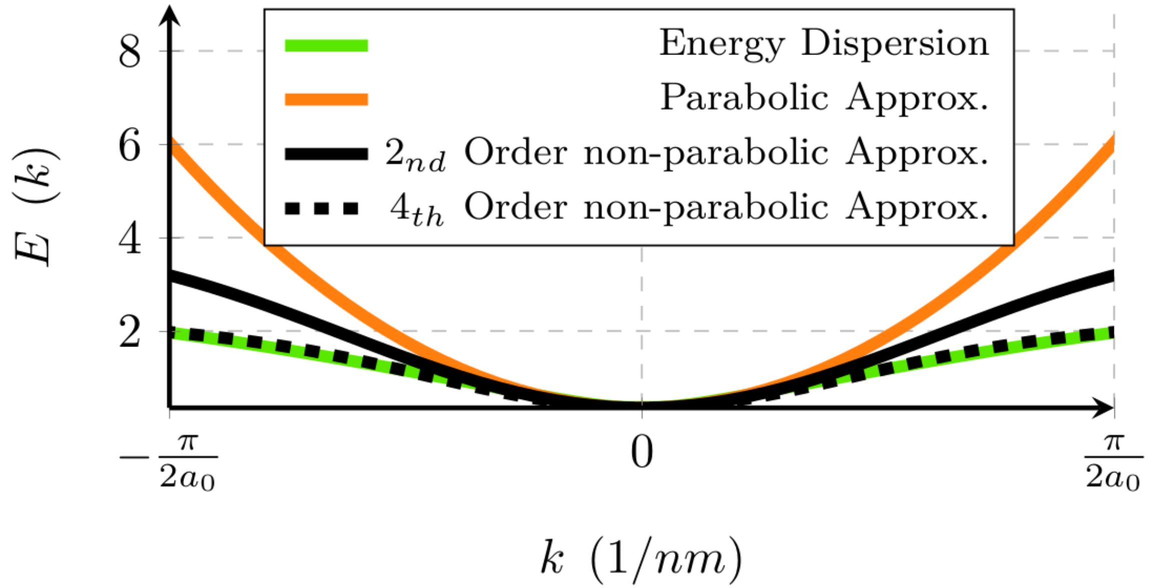

Fig. 12: Bulk energy dispersion in the Γ valley for InAs with parabolic, second order and fourth order approximations.

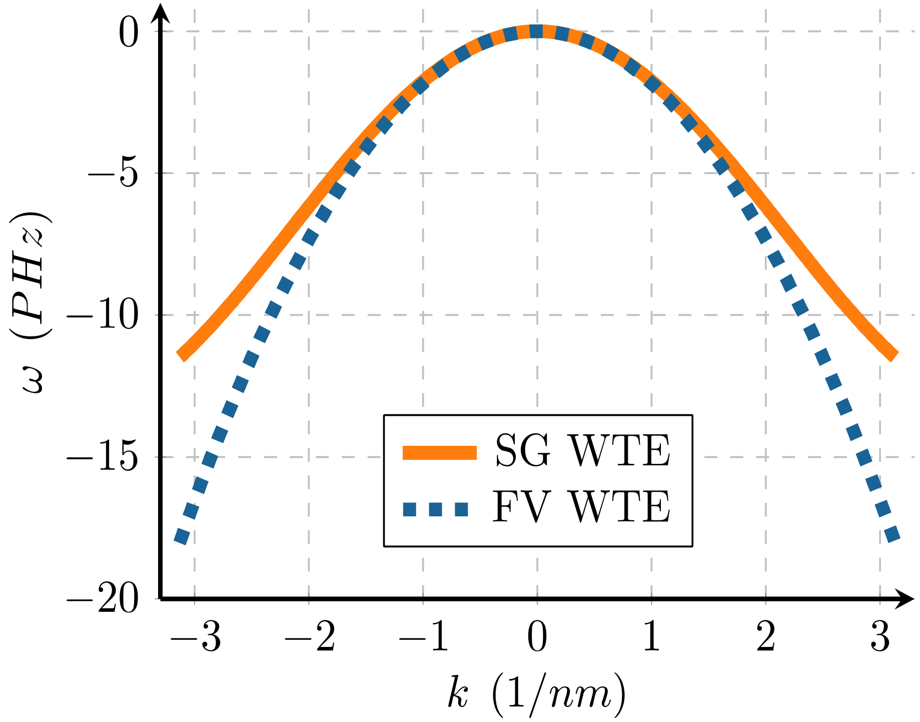

Fig. 13: The numeric dispersion for first order staggered grids and for a standard finite volume discretization of the Wigner Transport Equation.

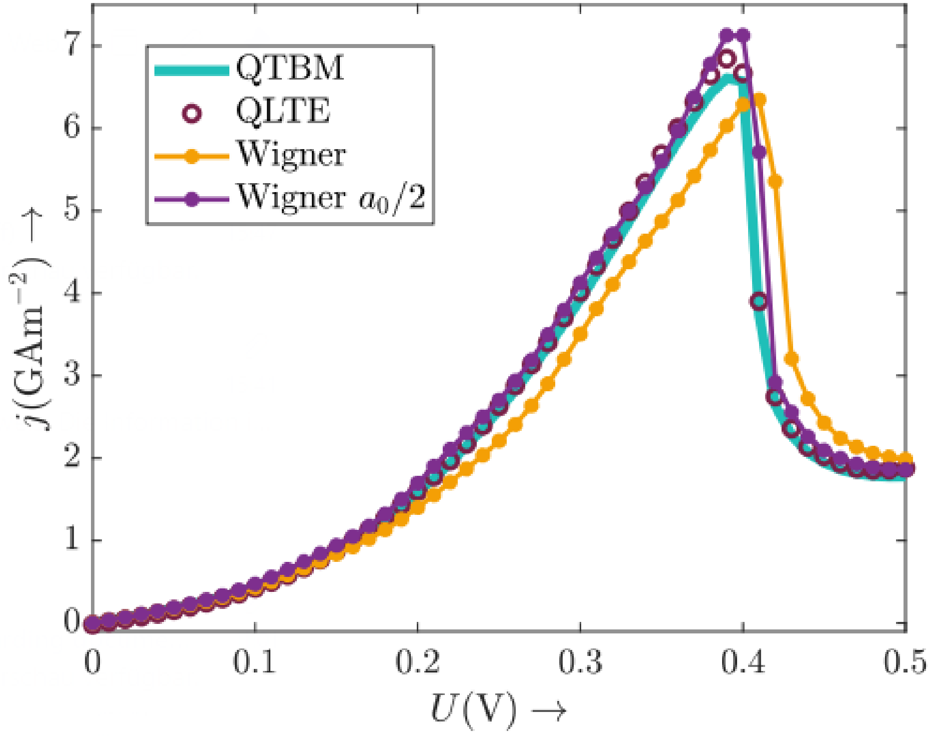

Fig. 14: Steady state I-V curves are shown applying the QTBM, the conventional WTE and the proposed approach (QLTE). The current density is shown dependent on the applied voltage U.

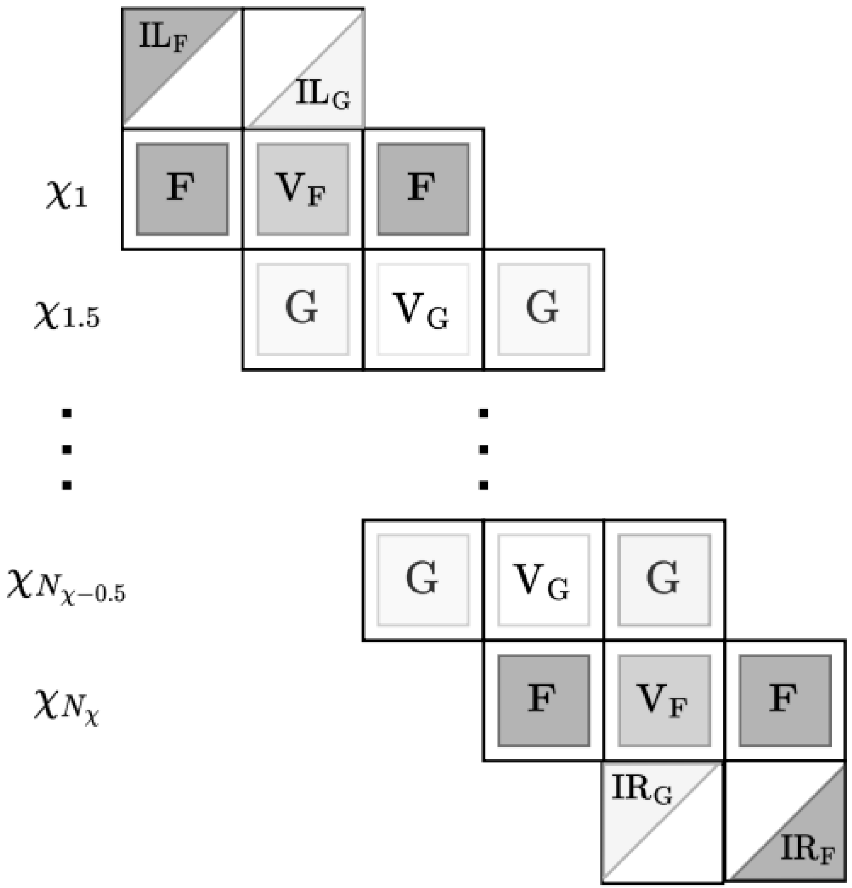
IL_F
IL_G
χ_1
F
V_F
F
$\chi_{1.5}$
G
V_G
G
$\chi_{N_{\chi-0.5}}$
G
V_G
G
χ_{N_χ}
F
V_F
F
IR_G
IR_F

Tight Binding formalism: Benefits

- ✓ Atomistic view (orbital functions)
- ✓ Simple Discretization
- ✓ No information loss
- ✓ Computationally efficient
- ✓ Heterostructures